

NMR Determination of the Bioactive Conformation of Peloruside A Bound To Microtubules

Jesús Jiménez-Barbero,^{*,†} Angeles Canales,[†] Peter T. Northcote,[‡] Rubén M. Buey,[†] José Manuel Andreu,[†] and J. Fernando Díaz^{*,†}

Contribution from the Centro de Investigaciones Biológicas, CSIC, Ramiro de Maeztu 9, 28040 Madrid, Spain, and Chemical and Physical Sciences, Victoria University of Wellington, Wellington, New Zealand

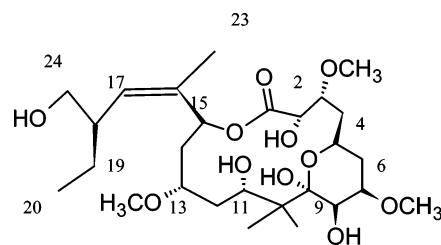
Received November 25, 2005; E-mail: jjbarbero@cib.csic.es; fer@cib.csic.es

Abstract: We report here on the determination of the conformation of Peloruside A bound to biochemically stabilized microtubules, by using TR-NOESY NMR experiments. As a previous step, the conformation of the free molecule in water solution has also been deduced. Despite the large size of the ring, Peloruside A mainly adopts two conformations in water solution. A conformational selection process takes place, and the microtubules-bound conformer is one of those present in the water solution, different than that existing in chloroform medium. A model of the binding mode to tubulin has also been proposed, by docking the bioactive conformation of peloruside, which involves the α -tubulin monomer, in contrast with taxol, which binds to the β -monomer.

Introduction

Microtubule stabilizing agents are a chemically diverse set of small molecules which bind to microtubules in different fashions¹ and block microtubule dynamics, leading to mitotic spindle impairment and cell apoptosis; several of them are antitumor drugs.² Most microtubule stabilizing agents bind at the paclitaxel binding site of β -tubulin.^{1,3} Current information on the bound conformations of paclitaxel or epothilone comes mainly from modeling based on incomplete electron crystallographic densities of nonmicrotubule tubulin zinc sheets^{4,5} or on partial data from solid-state NMR.⁶ In contrast to these compounds, laulimalide⁷ and peloruside⁸ apparently share a new binding site, different from the paclitaxel site and still to be mapped on the tubulin molecule, and retain activity in paclitaxel-resistant cells, which holds an important chemotherapeutic potential. Peloruside A (Scheme 1) is isolated from a New Zealand marine sponge.⁹

Scheme 1



The knowledge of the bioactive conformation of these molecules is of paramount interest for the derivation of analogues with improved activity.^{7b,10} A variety of conformational studies on paclitaxel, epothilones, and other tubulin acting molecules have been performed, both in the free and bound states.^{10,11} The identification of the configuration of the stereogenic centers of Peloruside A⁹ was followed by reports on the synthesis of some fragments¹² and the total synthesis together with the description of its absolute configuration.¹³ Moreover, some conformational features of Peloruside A (Figure 1) in chloroform solution have been deduced by using NMR.^{9,13}

We report here on the determination of the conformation of Peloruside A bound to biochemically stabilized microtubules,

[†] CSIC.

[‡] Victoria University of Wellington.

- (1) (a) Buey, R. M.; Barasoain, I.; Jackson, E.; Meyer, A.; Giannakakou, P.; Paterson, I.; Mooberry, S.; Andreu, J. M.; Diaz, J. F. *Chem. Biol.* **2005**, *12*, 1269–1279. (b) Diaz, J. F.; Strobe, R.; Engelborghs, Y.; Souto, A. A.; Andreu, J. M. *J. Biol. Chem.* **2000**, *275*, 26265–26276.
- (2) Wilson, L.; Jordan, M. A. *Nat. Rev. Cancer* **2004**, *4*, 253–265.
- (3) Lowe, J.; Li, H.; Downing, K. H.; Nogales, E. *J. Mol. Biol.* **2001**, *313*, 1045–1057.
- (4) Snyder, J. P.; Nettles, J. H.; Cornett, B.; Downing, K. H.; Nogales, E. *Proc. Natl. Acad. Sci. U.S.A.* **2001**, *98*, 5312–5316.
- (5) Nettles, J. H.; Li, H.; Cornett, B.; Krahn, J. M.; Snyder, J. P.; Downing, K. H. *Science* **2004**, *305*, 866–869.
- (6) Li, Y.; Poliks, B.; Cegelski, L.; Poliks, M.; Gryczynsky, Z.; Piszczek, G.; Jagtap, P. G.; Studelska, D. R.; Kingston, D. G. I.; Schaefer, J.; Bane, S. *Biochemistry* **2000**, *39*, 281–291.
- (7) (a) Pryor, D. E.; O'Brate, A.; Bilcer, G.; Diaz, J. F.; Wang, Y.; Kabaki, M.; Jung, M. K.; Andreu, J. M.; Gosh, A. K.; Giannakakou, P.; Hamel, E. *Biochemistry* **2002**, *41*, 9109–9115. (b) The conformational behavior of laulimalide in dimethyl sulfoxide solution has recently been described: Thepchatrri, P.; Cicero, D. O.; Montegudo, E.; Ghosh, A. K.; Cornett, B.; Weeks, E. R.; Snyder, J. P. *J. Am. Chem. Soc.* **2005**, *127*, 12838–12846.

- (8) Gaitanos, T. N.; Buey, R. M.; Diaz, J. F.; Northcote, P. T.; Teesdale-Spittle, P.; Andreu, J. M.; Miller, J. H. *Cancer Res.* **2004**, *64*, 5063–5067.
- (9) West, L. M.; Northcote, P. T.; Battershill, C. N. *J. Org. Chem.* **2000**, *65*, 445–449.
- (10) Jiménez-Barbero, J.; Amat-Güerri, F.; Snyder, J. P. *Curr. Med. Chem. Anticancer Agents* **2002**, *2*, 91–122 and references therein.
- (11) (a) Carlomagno, T.; Sanchez, V. M.; Blommers, M. J.; Griesinger, C. *Angew. Chem., Int. Ed.* **2003**, *42*, 2515–2517. (b) Carlomagno, T.; Blommers, M. J.; Meiler, J.; Jahnke, W.; Schupp, T.; Petersen, F.; Schinzer, D.; Altmann, K. H.; Griesinger, C. *Angew. Chem., Int. Ed.* **2003**, *42*, 2511–2515.
- (12) Paterson, I.; Di Francesco, M. E.; Kühn, T. *Org. Lett.* **2003**, *5*, 599–602.
- (13) Liao, X.; Wu, Y.; De Brabender, J. *Angew. Chem., Int. Ed.* **2003**, *42*, 1648–1652.

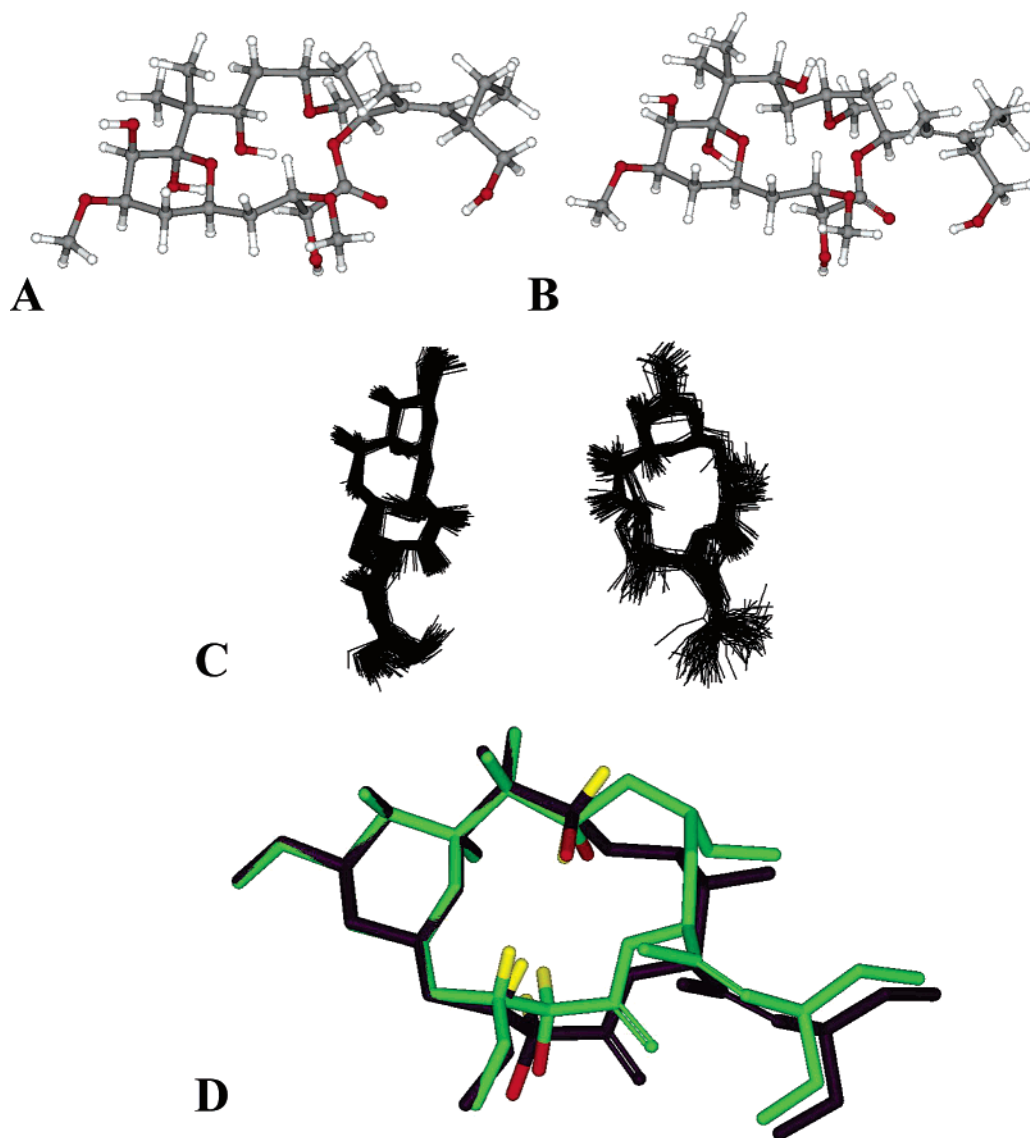


Figure 1. Conformational analysis of **1**. The two low energy conformations of Peloruside A in water solution. (A) The water conformer that is similar to the chloroform conformer. (B) The bioactive conformer. (C) The two major conformational families A and B were found to be **1** by the MC/EM conformational search. Superimposition of 100 snapshots taken from the two 5 ns of molecular dynamics simulations. (A) The bioactive conformer. (B) The last part of the trajectory starting from the chloroform conformer, A. After 4 ns, a transition to the bioactive B conformer is observed. (D) Superimposition of the two low energy conformations of Peloruside A in water solution. In green, conformer A. In black, conformer B. Key, H2, H3, and H11, hydrogens are shown in yellow, while O2 and O11 are in red.

by using TR-NOESY NMR experiments.¹⁴ As a previous step, the conformation of the free molecule in water solution has also been deduced by a combined protocol of NMR data, assisted by modeling procedures. Despite the large size of the ring, Peloruside A mainly adopts two conformations in water solution. A conformational selection process takes place, and the microtubules-bound conformer is one of those present in the water solution, different than that existing in chloroform medium.

Results and Discussion

NMR Studies of Free Peloruside A. NMR experiments in deuterated water solution were carried out at 500 MHz at temperatures ranging from 298 to 313 K. A complete assignment of the ¹H NMR resonance signals of Peloruside A (**1**) was achieved on the basis of TOCSY,¹⁵ HSQC,¹⁶ and T-ROESY¹⁷

experiments (see Supporting Information). The relevant NMR parameters (chemical shifts and coupling constants) are given in the Supporting Information. The analysis of some conformational features of this molecule in chloroform solution has been performed.^{9,13} The differences in chemical shifts and coupling constants between the reported data in the organic solvent and water are also given in the Supporting Information. Some differences are observed for the chemical shifts. The analysis of the vicinal proton–proton coupling constants for the six-membered ring indicates that it adopts a well-defined conformation.¹⁸ Generally speaking, no major changes were deduced for the coupling constant values between chloroform and water, except for the region around C11–C14. On a qualitative basis, these data seem to indicate the existence of a

(14) (a) Bothner-By, A. A.; Gassend, R. *Ann. N.Y. Acad. Sci.* **1973**, *222*, 668–676. (b) Ni, F. *Prog. NMR Spectrosc.* **1994**, *26*, 517–539.

(15) Braunschweiler, L.; Ernst, R. R. *J. Magn. Reson.* **1983**, *53*, 521–527.

(16) Bodenhausen, G.; Reuben, D. *J. Chem. Phys. Lett.* **1980**, *69*, 185–189.

(17) Hwang, T. L.; Shaka, A. J. *J. Am. Chem. Soc.* **1992**, *114*, 3157–3158.

(18) Haasnoot, C. A. G.; de Leeuw, F. A. A. M.; Altona, C. *Tetrahedron* **1980**, *36*, 2783–2794.

similar conformational behavior. NOE experiments were also performed. The intraresidue NOE cross-peaks for the six-membered ring, along with the J values, support that it adopts a chair conformation.

Regarding the global shape of the macrocycle, the relationship between NOE signals and proton–proton distances is well established¹⁹ and can be worked out at least semiquantitatively using a relaxation matrix.²⁰ The NOE intensities reflect the conformer populations, and therefore information on the population distributions in free solution can be obtained by focusing on the key NOEs that characterize the different possible conformations.

At 500 MHz and room temperature, all the cross-peaks observed in the NOE spectra of **1** in water solution were very weak. The $\omega\tau_c$ value is close to 1.1, providing an almost zero longitudinal NOE.²⁰ Thus, the basic information was derived from tilted ROESY experiments (T-ROESY, figures in Supporting Information) that provided the crucial cross-peaks that are reported in Table 1.

Modeling Studies of Free Peloruside A. Comparison with the NMR Results. The conclusions of the NMR experiments were validated by molecular mechanics and dynamics methods. To obtain a satisfactory geometry that would comply with the NMR-derived parameters, computational models of **1** were generated as described in the Experimental Section (MC/EM conformational searches and molecular dynamics simulations, MM3* force field²¹ in MacroModel,²² GB/SA water solvation²³) and compared to the experimental results. The calculations pointed to the presence of two conformational families, which mainly differ in the relative orientation of the C10 to C15 region (Figure 1A,B and Table 2).

One of these geometries (A) is in agreement with that postulated for Peloruside A in chloroform solution.^{9,13} From the steric energy viewpoint, and using MM3* as integrated in MacroModel 7.0, with the continuum GB/SA solvent model for water, conformer B is about 2 kcal mol⁻¹ more stable than A. The major energy component that stabilizes B is solvation energy. In fact, B is about 1 kcal mol⁻¹ more stable than A when the calculations are performed in vacuum, with a bulk dielectric constant of 1.5.

According to the MD simulations, each of these conformations is moderately flexible along the backbone (Figure 1C), with higher variation for the lateral chain. Indeed, the H2/H3 and H3/H4 coupling constant values indicate the presence of conformational averaging in this region since none of the extreme values for the “pure” A or B conformers may explain the experimental data. A similar conclusion may be deduced from the averaged H13/H14 coupling constant value.

An ensemble average of 300 conformers was taken from the molecular dynamics simulations carried out for each conformational family and was used to calculate the ensemble average distances for the relevant proton pairs (according to a $\langle r^{-1/6} \rangle^{-1/6}$).

(19) Neuhaus, D.; Williamson, M. P. *The NOE Effect in Structural and Conformational Analysis*; VCH: New York, 1989.

(20) See, for instance: *NMR Spectroscopy of Glycoconjugates*; Jiménez-Barbero, J., Peters, T., Eds.; Wiley-VCH: Weinheim, Germany, 2002.

(21) Allinger, N. L.; Yuh, Y. H.; Liu, J. H. *J. Am. Chem. Soc.* **1989**, *111*, 8551–8559.

(22) Mohamadi, F.; Richards, N. G. J.; Guida, W. C.; Liskamp, R.; Lipton, M.; Caufield, C.; Chang, G.; Hendrickson, T.; Still, W. C. *J. Comput. Chem.* **1990**, *11*, 440–467.

(23) Still, W. C.; Tempczyk, A.; Hawley, R.; Hendrickson, T. *J. Am. Chem. Soc.* **1990**, *112*, 6127–6129.

Table 1. Principal NOE Contacts for Peloruside A in the Free State^a

proton pair	observed NOE intensity (free state, D ₂ O)	NOE-based ^b experimental r (Å)	MM3*-based ensemble average distance (conformer B)	MM3*-based ensemble average distance (conformer A)
H2 H3	strong	2.5	2.5	2.5
H2 H5	strong	2.4	2.1	2.3
H2 H12A	weak	3.1	2.6	5.3
H2 H11	N.O.	> 4	5.3	2.8
H3 H12A	weak	3.3	3.2	4.9
H3 H11	very weak	3.8	4.6	2.5
H3 OMe3	medium	2.9	3.5	3.3
H5 H6B	strong	2.5	2.5	2.5
H5 H6A	medium weak	3.0	3.1	3.1
H5 H4A	strong	2.5	2.5	2.4
H6A H4B	strong	2.5	2.5	2.5
H6B H7	strong	2.5	2.5	2.5
H7 H8	strong	2.5	2.5	2.5
H7 OMe7	strong	2.5	2.6	2.7
H8 H21	medium	2.9	3.0	3.2
H8 H22	medium strong	2.7	2.7	2.7
H8 OMe7	medium	2.9	3.3	3.2
H11 H21	strong	2.6	2.7	2.7
H11 H22	strong	2.6	2.7	3.9
H11 H13	medium weak	3.0	2.4	3.8
H11 OMe13	very weak	3.5	4.7	4.9
H12A H14A	medium	2.9	3.1	2.4
H12B H22	strong	2.4	2.4	2.5
H13 H14A	medium	2.9	2.6	2.7
H13 H14B	strong	2.4	2.4	2.2
H13 H12B	medium strong	2.6	2.5	2.4
H13 OMe13	medium strong	2.6	2.5	2.5
H13 H12A	weak	3.0	3.1	2.6
H14B H15	strong	2.5	2.5	3.0
H14A H23	medium	2.7	2.5	2.6
H15 OMe13	medium	2.9	3.0	2.5
H15 H18	strong	2.4	2.1	2.2
H17 H19A	medium strong	2.6	2.6	2.7
H17 H20	weak	3.1	4.1	3.9
H17 H23	strong	2.5	2.7	2.8
H17 H24A	medium strong	2.6	2.6	2.7
H18 H19B	strong	2.5	2.6	2.8
H18 OMe13	medium	2.9	3.3	3.1
H18 H20	strong	2.5	2.6	2.6
H18 H24B	medium strong	2.7	2.6	2.5
H19B OMe13	medium strong	2.7	3.6	2.8
H20 H14B	medium	2.9	4.2	4.1
H23 OMe13	weak	3.1	5.7	4.6
H24B H20	weak	3.1	3.0	2.9

^a The experimental distances (r , Å; $\pm 10\%$) are estimated according to a full matrix relaxation approach from a build up curve analysis of the T-ROESY data.^{19,20} The intraresidue H–H distances within the six-membered ring were taken as internal reference. ^b From a full matrix relaxation approach. N.O. = no observable NOE contact.

Table 2a. Torsion Angle Values for the Two Major Conformers of Peloruside A from MM3* Calculations

torsion angle	A	B	torsion angle	A	B
C1–C2–C3–C4	170	166	C13–C14–C15–O	–67	–63
C2–C3–C4–C5	–57	–60	C14–C15–O–C1	173	167
C3–C4–C5–C6	–161	–173	C15–O–C1–C2	–179	–171
C4–C5–C6–C7	173	176	O–C1–C2–C3	–67	–59
C5–C6–C7–C8	–53	–55	C14–C15–C16–C17	–112	–101
C6–C7–C8–C9	55	56	C15–C16–C17–C18	–2	0
C7–C8–C9–C10	180	–179	C16–C17–C18–C19	104	115
C8–C9–C10–C11	173	171	C17–C18–C19–C20	–175	–174
C9–C10–C11–C12	175	56	C17–C18–C24–O	55	56
C10–C11–C12–C13	177	159	C2–C3–O–CH3	–84	–87
C11–C12–C13–C14	–66	64	C6–C7–O–CH3	–74	–74
C12–C13–C14–C15	105	71	C12–C13–O–CH3	147	159

These distances (and those corresponding to the experimental data, calculated according to a full relaxation matrix approach) were compared to the experimental ones (see Table 1). It can be seen that the NOE data cannot be explained by any of the

Table 2b. Comparison between the Experimental Values of J Couplings in Water Solution (this work) and Those Reported for Peloruside A in Chloroform Solution⁹ (the comparison with the calculated J couplings for the MM3*-based conformers, according to the generalized Karplus equation proposed by Altona and co-workers,¹⁸ is also given^a

torsion angle	$J_{\text{EXP}} (\text{D}_2\text{O})$	$J_{\text{EXP}} (\text{CDCl}_3)$	J_{confB}	J_{confA}^b	torsion angle	$J_{\text{EXP}} (\text{D}_2\text{O})$	$J_{\text{EXP}} (\text{CDCl}_3)$	J_{confA}	J_{confB}^b
H2/H3	1.6	0.5	0.5	0.3	H12A/H13		10.5	5.0	11.4
H3/H4A	9.7	10.5	11.4	11.6	H12B/H13			1.8	3.7
H3/H4B	5.1	5.5	3.9	3.5	H13/H14A		1.5	1.7	1.3
H4A/H5	2.5	2.5	4.0	2.6	H13/H14B	7.5	11.5	9.4	6.0
H4B/H5	11.0	11.0	11.3	11.7	H14A/H15	11.6	10.0	11.4	11.4
H5/H6A	-	12.0	11.7	11.7	H14B/H15	1.7	1.0	1.3	1.3
H5/H6B	3.3	2.5	2.5	2.5	H17/H18	10.3	10.0	11.0	11.6
H6A/H7	11.6	11.5	11.0	11.2	H18/H19A	2.9		2.4	2.4
H6B/H7	4.3	5.2	5.1	4.8	H18/H19B	8.4		12.3	12.3
H7/H8	2.5	3.0	2.6	2.5	H18/H24A	6.0	4.0	4.6	4.5
H11/H12A	9.6	10	11.4	9.9	H18/H24B	7.1		11.7	11.8
H11/H12B	2.3		1.5	1.8					

^a The values in bold indicate the presence of conformational averaging in water solution. ^b From ref 1.

two conformations if they are considered to be the unique one present in solution. It is necessary to consider both A and B geometries to account for the experimental NOE data, especially when considering the NOEs between the H2, H3, H11, H12, and H13 hydrogens (see Table 1). In particular, conformer A shows close proximity between H2/H11 and H3/H11 proton pairs (as reported in chloroform solution^{9,13}), while both H2 and H3 are relatively far from H12A (more than 4.5 Å apart). In contrast, conformer B (Table 1) shows the opposite situation, with close proximity between H2/H12A and H3/H12a proton pairs, while both H2 and H3 are relatively far from H11 (more than 4.5 Å apart). Weak cross-peaks are observed between H2/H12A and H3/H12a proton pairs, while a very weak one is detected just above the noise level for H3/H11. In addition, a medium weak cross-peak is shown for H11/H13 that is in agreement with the presence of conformer B. These observations permit one to deduce that the proposed major conformer in chloroform solution (conformer A^{9,13}) is not the predominant one in water solution. A combination of both A and B conformers better explains the data in D₂O. In any case, the presence of conformational mobility around this region is granted since the key NOEs are indeed weak, in contrast with the expectations for a single well-defined conformation. Regarding the C18/C19 and C18/C24 torsions, both the coupling and NOE data are also in agreement with a conformational equilibrium between two major conformers at either linkage (figure in the Supporting Information), while the NOE data are also in agreement with particular orientations of the OMe groups, with OMe13 primarily pointing toward H15, OMe7 toward H8, and OMe3 toward H4. A key point that differentiates both conformers in the relative orientation between O11 and O13 is that conformer A (see Figure 1A) permits the establishment of a hydrogen bond in which O13 is accepting hydrogen from OH11. However, the arrangement in conformer B is rather different, and this intramolecular hydrogen bond is no longer possible for geometry B. Possibly, the presence of water molecules competes with this intramolecular hydrogen bonding. Thus, the conformational behavior of Peloruside A in water solution can be described by a conformational equilibrium between two geometries (Figure 1) which are similar along the C1 to C9 region but differ on the torsional angles (Table 2) along the C10 to C15 section. Both sets of geometries show restricted flexibility along their torsional degrees of freedom (Figure 1C), as suggested by the MD simulations. According to the NOE data, conformer B is somehow more populated than A in water

solution, but in a rather small extent. A superimposition between the two geometries is shown in Figure 1D.

NMR TR-NOESY Studies of Peloruside A in the Presence of Microtubules. As a further step, the bioactive conformation of Peloruside A, bound to microtubules, was elucidated. As previously shown, for ligands which are not bound tightly and exchange between free and bound state at a reasonably fast rate, the transferred nuclear Overhauser enhancement (TR-NOESY) experiment provides an adequate means to determine the conformation of the bound ligand.^{14,24} Within this context, it is noteworthy to mention seminal methodological reports by Griesinger, Carlomagno, and co-workers, who described¹¹ the bound conformation of epothilone to tubulin, using a combination of transferred NOESY and transfer of cross-correlated relaxation experiments, with a C13-labeled synthetic epothilone. In our case, no labeled compound was used, and the TR-NOESY approach was enough to deduce the bioactive conformation of Peloruside A. Regarding the above-mentioned work on bound epothilones,¹¹ the authors employed dialyzed and lyophilized tubulin that was dissolved in regular D₂O prior to each measurement.¹¹ It is well-known that purified tubulin is labile and denatures rapidly in solution, and that it is usually inactive after dialysis or lyophilization in the absence of stabilizing cosolvents.²⁵ This fact casts doubt on the specificity of any ligand interactions observed with such dialyzed and lyophilized tubulin preparations, unless they are shown to be active in microtubule assembly. Even if that was the case, tubulin in plain D₂O does not assemble into microtubules. It has been described that the microtubule taxoid binding site does not exist in dimeric tubulin, at least with an affinity higher than millimolar.²⁶ Although epothilones might bind with low affinity to un-assembled tubulin,²⁷ it is not possible to ensure that epothilone under the reported conditions¹¹ is indeed bound to the same site as in native microtubules; therefore such drug-protein interactions observed, if specific, would be weakly representative of the biomedically relevant ones. Thus, we rather preferred to search for biochemical conditions in which stable microtubules are assembled from native tubulin with GMPCPP. The micro-

- (24) (a) See, for instance: Bevilacqua, V. L.; Thomson, D. S.; Prestegard, J. H. *Biochemistry* **1990**, *29*, 5529–5537. (b) Bevilacqua, V. L.; Kim, Y.; Prestegard, J. H. *Biochemistry* **1992**, *31*, 9339–9349.
(25) (a) Andreu, J. M. In *Methods in Molecular Medicine*; Zhou, J., Ed.; Humana Press: Totowa, NJ, 2005. (b) Lee J. C. *Methods Cell Biol.* **1982**, *24*, 9–30.
(26) Diaz, J. F.; Andreu, J. M. *Biochemistry* **1993**, *32*, 2747–2755.
(27) Buey, R. M.; Diaz, J. F.; Andreu, J. M.; O'Brate, A.; Giannakakou, P.; Nicolaou, K. C.; Sasmal, P. K.; Ritzen, A.; Namoto, K. *Chem. Biol.* **2004**, *11*, 225–236.

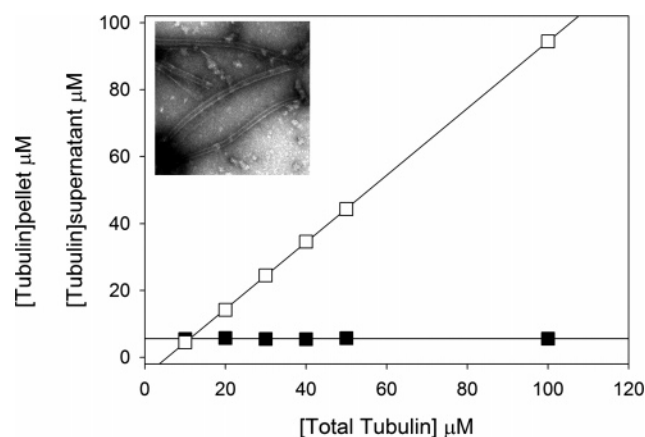


Figure 2. Polymerization of tubulin in 10 mM sodium phosphate, 6 mM MgCl_2 buffer, 0.1 mM GMPCPP pH 6.7 buffer at 37 °C, as measured by sedimentation. Pelleted tubulin (empty squares), tubulin in the supernatant (filled squares). Inset: electron micrograph of the microtubules assembled in GMPCPP containing buffer.

tubulin–peloruside NMR samples were examined by electron microscopy and found to consist of microtubules (see Figure 2 and Experimental Section for details).

The addition of the microtubules solution to a NMR tube containing **1** induced broadening of the resonance signals in the ^1H NMR spectrum, indicating that binding occurs. TR-NOESY experiments were then performed on the ligand: microtubule sample at different mixing times. Negative cross-peaks were clearly observed at 303 K, as expected for ligand binding (Figure S1 in the Supporting Information), in contrast with the observations for the free ligand, for which no NOEs were observed in the free state (zero crossing in the NOE curve). Thus, although in principle, TR-NOESY data could be safely used to deduce the bioactive conformation of this key molecule, the obtained data should be taken with caution due to the following reasoning. One of the major difficulties with TR-NOESY data is the fact that, in general, it is not possible to retrieve data from tight binding sites (very low dissociation rates), and data from minor (weak or nonspecific) binding sites may dominate. The equilibrium dissociation constant of peloruside to stabilized microtubules is ca. 0.4 μM , estimated from sedimentation and HPLC measurements (Diaz, J. F.; Paterson, I. unpublished results). Unfortunately, it is not possible to quantitatively deduce the kinetic dissociation rate of Peloruside A from microtubules without the knowledge of the kinetic scheme of binding for this molecule. Indeed, binding of microtubule stabilizing agents to the taxoid binding site to microtubules is a complex process involving at least three kinetic steps.^{1a} Thus, our data should be taken within this caution. STD experiments were also performed to try to deduce the binding epitope of peloruside when bound to microtubules. Indeed, with low saturation times (below 500 ms), the protons in the periphery of the macrocyclic ring were observed, namely H2, H8, H17, and H19 to H24, as well as those belonging to the three methoxy rings (figure in the Supporting Information). For longer saturation times, all the peloruside protons were observed.

From the TR-NOESY data, for bound **1**, the orientation of the six-membered ring moiety relative to the backbone is also almost identical to that observed in the free state, as shown by the key short contacts H2/H5 (Table 3). Also, the analysis of the TR-NOESY cross-peaks, using a full relaxation matrix

Table 3. Analysis of the Estimated Interproton Distances for Peloruside A in the Tubulin Bound State^a

proton pair		observed intensity bound state	deduced r (Å) CORCEMA analysis	MM3 ⁺ -based ensemble average distance (B)
H2	H3	strong	2.5	2.5
H2	H5	very strong	2.3	2.1
H2	H12A	medium	2.8	2.6
H2	H11	N.O.	>4	5.3
H3	H12A	medium	2.8	3.2
H3	H11	N.O.	>4	4.6
H3	OMe3	strong	2.9	3.5
H6B	H7	strong	2.5	2.5
H7	H8	strong	2.5	2.5
H7	OMe7	strong	2.5	2.6
H8	H21	strong	2.6	3.0
H8	H22	strong	2.6	2.7
H8	OMe7	strong	2.7	3.3
H11	H21	strong	2.5	2.7
H11	H22	strong	2.5	2.7
H11	H13	strong	2.6	2.4
H11	OMe13	medium	2.9	4.7
H12B	H22	strong	2.4	2.4
H13	OMe13	medium strong	2.6	2.5
H14A	H23	medium strong	2.6	2.5
H15	OMe13	medium	2.9	3.0
H15	H18	very strong	2.2	2.1
H17	H19A	medium strong	2.7	2.6
H17	H20	medium	2.8	4.1
H17	H23	strong	2.5	2.7
H17	H24A	medium strong	2.6	2.6
H18	H19B	strong	2.5	2.5
H18	OMe13	medium	2.9	3.3
H18	H20	very strong	2.4	2.6
H18	H24B	strong	2.6	2.6
H19B	OMe13	medium strong	2.7	3.6
H20	H14B	weak	3.9	4.2
H23	OMe13	medium	3.0	5.7
H24B	H20	weak	3.1	3.0

^a The experimental distances (r , Å; $\pm 15\%$) are estimated according to a full matrix relaxation approach from a CORCEMA-based²⁸ analysis of the TR-NOESY data. The intraresidue H–H distances within the six-membered ring were taken as internal reference. N.O. = no observable NOE contact.

approach, with the help of the CORCEMA program,²⁸ permitted us to deduce that the relative orientation of the C1–C5 macrocycle remains unalterable upon binding. Regarding the C9–C15 section, both H2 and H3 give clear cross-peaks to H12A, while no cross-peaks are observed between H2 and H3 to H11. Moreover, the H11/H13 is strong.

The TR-NOESY data are also in agreement with the major orientations of the OMe groups similar to those described for the free state. T-ROESY experiments allowed us to exclude spin diffusion effects for these key cross-peaks.²⁹ Thus, the observed pattern is that expected for a bound B conformer, with no evidence of binding for the chloroform conformer by the microtubules. Indeed, the observed cross-peaks are in agreement with a major B conformation in the bound state, indicating the existence of a conformational selection process. A view of the polar and nonpolar surfaces of conformer B is shown in Figure 3, while those for A are shown in the Supporting Information.

Docking. Finally, to have a three-dimensional picture of the interactions, the experimentally derived NMR conformation was

- (28) (a) Moseley, H. N. B.; Curto, E. V.; Krishna, N. R. *J. Magn. Reson., Ser. B* **1995**, *108*, 243–261. (b) Krishna, N. R.; Moseley, H. N. B. *Biol. Magn. Reson.* **1999**, *17*, 223–307.
- (29) (a) Asensio, J. L.; Cañada, F. J.; Jimenez-Barbero, J. *Eur. J. Biochem.* **1995**, *233*, 618–630. (b) Arepalli, S. R.; Glaudemans, C. P. J.; Bax, A. *J. Magn. Reson.* **1995**, *106*, 195–199.

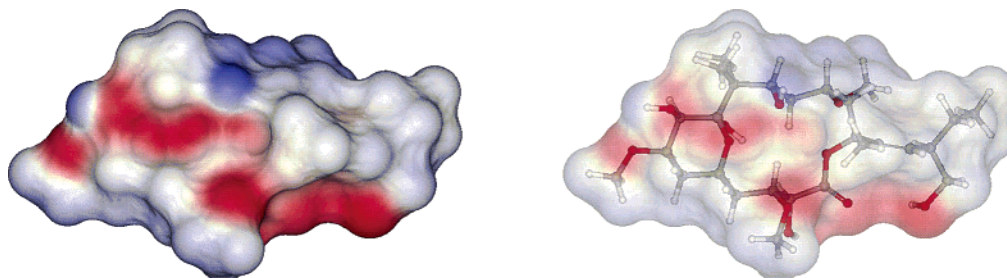


Figure 3. Representation of the polar and nonpolar areas of the bound conformer (B) of Peloruside A by microtubules. Conformer B seems to have a well-defined patch of polar and nonpolar areas.

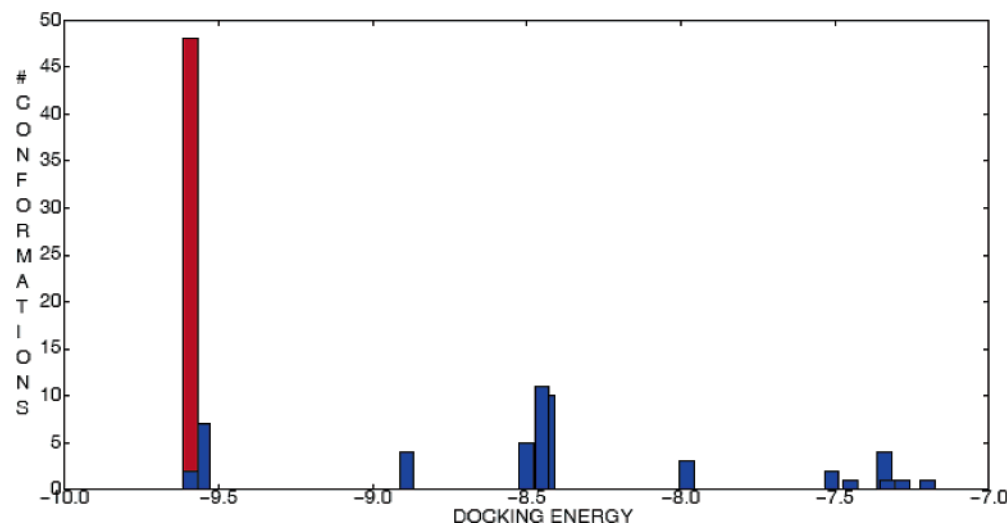


Figure 4. Histogram of the local docking for α -tubulin. Solutions that were within 0.5 Å RMS deviation of each other belonged to the same cluster, and the clusters were ranked according to their lowest energy member.

docked onto the α/β -tubulin dimer. The crude coordinates were first refined by using molecular dynamics simulations with the GROMOS96 43A1 force field³⁰ on the deposited coordinates of tubulin (pdb code: 1TUB)³¹ at the Protein Data Bank.³² Then, the docking was performed by using the AUTODOCK program.³³

First, a global search for binding sites in the α/β -tubulin dimer was carried out, with a grid spacing of 0.6 Å. Since all the binding modes obtained in this calculation were located at the region of α -tubulin that faces inside the microtubule (Figure 5A), the second step involved a local search for the α -tubulin monomer, with a grid spacing of 0.375 Å. Nevertheless, a local search located in β -tubulin was also performed (see below) for the sake of completeness.

The local docking for α -tubulin suggested that there is a preferred peloruside binding region within this monomer since 47 out of 100 structures could be gathered in the lowest energy cluster (Figure 4). In fact, this binding site is boxed in by loops S9–S10 and H1–S2, while the bottom side of the binding is mainly made up by helix H7 (Figure 5B). The loop between S9 and S10, which forms part of the intermediate domain, includes an eight-residue insertion in the α subunit which

occludes the site that is occupied by taxol in β -tubulin³¹ (compare panel B to panel C in Figure 5), while the H1–S2 loop is part of the N-terminal, nucleotide binding domain. H7 helix is a long α -helix that connects both domains. This potential binding site is close to that proposed by other authors.³⁵

There are a variety of nonpolar intermolecular contacts, while no key electrostatic interactions are established between peloruside and tubulin. Nevertheless, according to this binding mode, there are several hydrogen bonds of the ligand with residues GLU22, CYS25, THR361, and ARG320 (the latter being a residue from the S8–H10 loop; Figure 5B). In addition, there is a CH π -stacking interaction between the C20 methyl group of peloruside and the aromatic ring of PHE 244 (the coordinates of the modeled peloruside–tubulin complex are available from the authors upon request). The proposed model might clarify the way in which the laulimalide-like microtubule stabilizing agents indeed operate. Interestingly, in our model, peloruside does not seem to directly contact, in α -tubulin, with the equivalent loop of the key β -tubulin's M-loop (as in the case of taxol,³⁴ Figure 5C). This M-loop has been shown to be a key element of the lateral interactions between microtubule protofilaments.³⁶ This evidence suggests the possibility that the so-called laulimalide site ligands could stabilize microtubules by blocking tubulin in its straight polymerized conformation,³⁷

(30) Van Gunsteren, W. F.; Billeter, S. R.; Eising, A. A.; Hünenberger, P. H.; Krüger, P.; Mark, A. E.; Scott, W. R. P.; Tironi, I. G. *Biomolecular Simulation: The GROMOS 96 Manual and User Guide*; BIOMOS b.v.: Zürich, 1997.

(31) Nogales, E.; Wolf, S. G.; Downing, K. H. *Nature* **1998**, *391*, 199–203.

(32) The Protein Data Bank (www.rcsb.org/pdb); Berman, H. M.; Westbrook, J.; Feng, Z.; Gilliland, G.; Bhat, T. N.; Weissig, H.; Shindyalov, I. N.; Bourne, P. E. *Nucleic Acids Res.* **2000**, *28*, 235–242.

(33) Morris, G. M.; Goodsell, D. S.; Halliday, R. S.; Huey, R.; Hart, W. E.; Belew, R. K.; Olson, A. J. *J. Comput. Chem.* **1998**, *19*, 1639–1647.

(34) Nogales, E.; Whittaker, M.; Milligan, R. A.; Downing, K. H. *Cell* **1999**, *96*, 79–88.

(35) Pineda, O.; Farras, J.; Maccari, L.; Manetti, F.; Botta, M.; Vilarrasa, J. *Bioorg. Med. Chem. Lett.* **2004**, *14*, 4825–4829.

(36) Li, H.; DeRosier, D. J.; Nicholson, W. V.; Nogales, E.; Downing, K. H. *Structure* **2002**, *10*, 1317–1328.

(37) Amos, L. A.; Lowe, J. *Chem. Biol.* **1999**, *6*, R65–R69.

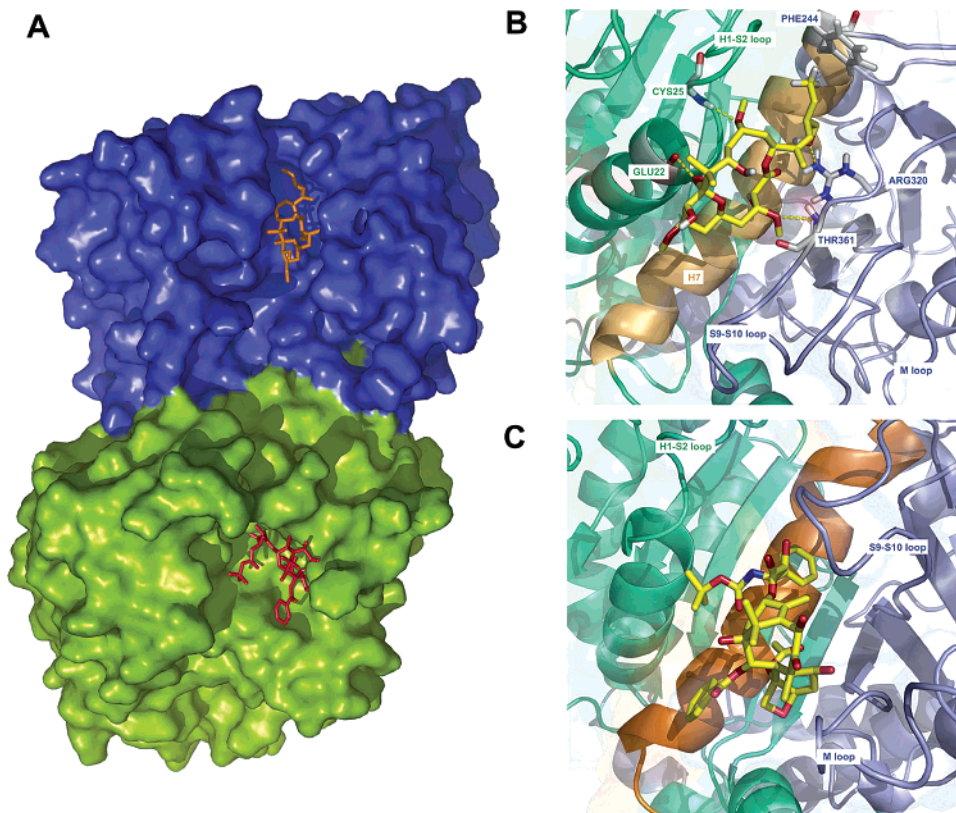


Figure 5. Predicted binding site for peloruside in the tubulin dimer. (A) Surface representation (view from the inner side of the microtubule) of a tubulin dimer with taxol (red) bound to β -tubulin (green) and peloruside (orange) bound to the predicted site in α -tubulin (blue). (B) View of the peloruside binding site. Hydrogen bonds are represented as yellow dashed lines, and the residues involved in these bonds are labeled. Some secondary structure elements are also labeled. (C) View of the taxol binding site. Some secondary structure elements are labeled. In panels B and C, H7 is colored in orange, and the N-terminal and intermediate domains are colored in green and blue, respectively.

rather than stabilizing lateral contacts between protofilaments, as it has been previously proposed for taxol.³⁶ Since peloruside, according to our proposed model, makes extensive contacts with the intermediate domain, the N-terminal domain, and the H7 helix, it could easily achieve the stabilization of microtubules by blocking the motions of the two described domains. This feature seems to be required for adopting the so-called curved—unassembled—conformation, thus blocking the intermediate domain rotation observed between both conformations.³⁸

On the other side, the histogram obtained in the local search performed for β -tubulin is shown in Figure S7 in the Supporting Information. The structures found for the most populated clusters were located in the nucleotide binding site of β -tubulin. Since this site is effectively occupied and occluded in the microtubule,³⁴ it cannot be considered as a true peloruside binding site. Additionally, peloruside also docked into the taxol binding site, but this mode was only present in the marginally populated clusters.

Conclusions

Our NMR data, assisted by molecular mechanics calculations, indicate that microtubules prefer to recognize the B conformer of peloruside A, which shows a clear distribution of polar and nonpolar surfaces.

Nevertheless, despite the large size of the macrocyclic ring, intramolecular interactions within the Peloruside A ring strongly

affects the conformational features of this molecule, which indeed only shows conformational mobility around a fairly narrow part of the molecule. Specifically, van der Waals contacts and torsional constraints strongly bias its conformational behavior. Yet, this existing conformational freedom, in the presence of a given solvent, serves to modulate the presentation of polar and nonpolar surfaces to interact with the binding site. Indeed, according to our experimental data, only one of the two major conformations existing in the water solution is bound to microtubules, distinct from that predominantly present in nonpolar (chloroform) solvents. A model of the binding mode to tubulin has also been proposed, which involves the α -tubulin monomer, in contrast with taxol, which binds to the β -monomer.

This experimental determination of the conformation of Peloruside A when bound to microtubules in solution should be helpful for the design of microtubule stabilizing agents with improved activity.

Experimental Section

Protein and Chemicals. Purified calf brain tubulin and chemicals were as described.²⁶ Peloruside A was isolated from the marine sponge, *Mycale hentscheli*, collected in Pelorus Sound off the northern coast of the South Island, New Zealand.⁹ The compound was diluted in DMSO to a final concentration of 10 mM and stored at -20 °C.

Preparation of the Sample for the TR-NOE Experiments. It is known that it is possible to assemble tubulin into microtubules in the absence of microtubule stabilizing agents by using unspecific assembly inductors, such as DMSO or glycerol. Since trace amounts of these nondeuterated promoters produce large proton signals in the NMR

(38) Ravelli, R. B.; Gigant, B.; Curmi, P. A.; Jourdain, I.; Lachkar, S.; Sobel, A.; Knossow, M. *Nature* **2004**, *428*, 198–202.

spectrum, we decided to employ a specific stabilizer. On this basis, we chose a slowly hydrolyzable nucleotide analogue, guanosine 5'-(α,β -methylene)triphosphate (GMPCPP).³⁹ GTP-bound tubulin in 10 mM sodium phosphate buffer, with 6 mM MgCl₂, H₂O, and 1 mM GTP at pH 6.4, is unable to assemble into microtubules at concentrations up to 200 μ M.²⁶ However, when GTP is substituted by GMPCPP (10 mM sodium phosphate, 6 mM MgCl₂ buffer, 0.1 mM GMPCPP buffer pH 6.7), tubulin assembles into microtubules with a critical concentration⁴⁰ of 5.6 μ M at 37 °C (Figure 4). If sodium is substituted by potassium in the buffer, the critical concentration is lower (4.6 μ M at 37 °C). A 10 mM potassium phosphate, 6 mM MgCl₂ buffer, 0.1 mM GMPCPP D₂O buffer, pD 6.4 was then chosen for the NMR experiments. The microtubule–peloruside NMR samples were examined by electron microscopy and found to consist of microtubules (inset, Figure 4)

Thus, the protein was equilibrated in 10 mM potassium phosphate, 6 mM magnesium chloride, 0.1 mM GMPCPP buffer in D₂O 99.9% (Merck) pD 6.4 by a two-step procedure. Sucrose and GTP were removed by a drained centrifuge column of Sephadex G-25 (6 \times 1 cm) equilibrated in 10 mM potassium phosphate, 10 μ M GTP buffer in D₂O 99.9% (Merck) pD 6.4, followed by a second chromatography in a cold Sephadex G-25 column equilibrated in 10 mM potassium phosphate, buffer in D₂O 99.9% (Merck) pD 6.7, and then 6 mM magnesium chloride and 0.1 mM GMPCPP were added to the solution, to give a pD 6.4. Immediately before performing the experiments, the protein concentration was adjusted to 20 μ M, the desired amount of Peloruside A was added to give the final 200 μ M concentration, and the sample was incubated for 30 min at 298 or 310 K (depending on the temperature of the experiment), the sample was found to be stable (as judged by the morphology of the polymers and the amount of protein pelleted by centrifugation) for more than 12 h. Under these conditions, the critical concentration of tubulin is 1.5 μ M at 298 K and 0.9 μ M at 310 K. This fact means that either 92.5 or 95.5% of the sample (at 298 or 310 K, respectively) is assembled into microtubules. Part of the formed polymers was adsorbed onto Formvar/carbon-coated 300 mesh copper grids, negatively stained with 1% uranyl acetate, and observed with an STEM LEO 910 transmission electron microscope (Zeiss Oberkochen, Germany) and found to consist of microtubules.

Computational Methods

Conformational Search and Dynamics of Peloruside A. The calculations were performed using the MacroModel/Batchmin²² package (version 7.0) and the MM3* force field.²¹ Bulk water solvation was simulated using MacroModel's generalized Born GB/SA continuum solvent model.²³ The conformational searches were carried out using 20 000 steps of the usage directed MC/EM procedure. Extended nonbonded cutoff distances (a van der Waals cutoff of 8.0 Å and an electrostatic cutoff of 20.0 Å) were used.

For the MC/SD⁴¹ dynamic simulations, van der Waals and electrostatic cutoffs of 25 Å, together with a hydrogen bond cutoff of 15 Å, were used. The dynamic simulations were run using the MM3* force field. Charges were taken from the force field. The same degrees of freedom of the MC/EM searches were used in the MC/SD runs. All simulations were performed at 300 K, with a dynamic time step of 1 fs and a frictional coefficient of 0.1 ps⁻¹. Two runs of 5 ns each were performed, starting from the two major conformations of the substrates, selected from the MC/EM outputs. The Monte Carlo acceptance ratio was about 2%, and each accepted MC step was followed by an SD step. Structures were sampled every 1 ps and saved for later evaluation. Monitoring both energetic and geometrical parameters checked convergence.

Molecular Dynamics Simulations and Docking Calculations.

Docking of Peloruside A was performed using the AutoDock 3.0 program.³³ During an AutoDock 3.0 simulation, multiple Lamarckian Genetic Algorithm runs occurred, each one providing one predicted binding mode, and cluster analysis was performed at the end of the simulation. Atomic coordinates for Peloruside A (B conformer) were obtained from the NMR data assisted by molecular mechanics calculations (see above). The α,β -tubulin dimer coordinates were obtained by molecular dynamics simulations using GROMOS96 software package,³⁰ which was obtained from BIOMOS b. v. (Zurich, Switzerland). The starting structure³¹ (1TUB) was taken from the Protein Data Bank,³² and an energy minimization of the protein with the two nucleotides and counterions in a rectangular water box (78.5 \times 87.0 \times 119.5) was performed using the same flowchart and parameters as previously described.⁴² Root-mean-square deviation (rmsd) of α -carbons in the resulting energy minimized structure with respect to those in the starting PDB structure was 0.62 Å. The velocities of the atoms were then randomly assigned to a Maxwell–Boltzmann velocity distribution at 300 K and, a 350 ps molecular dynamics simulation was performed using a constant pressure of 1 atm and a constant temperature of 300 K as described.⁴² The calculations were performed using the parallelized version of *promd* (GROMOS96) over 8 MIPS R14000 processors in a Silicon Graphics Origin 3800 workstation. After approximately 250 ps of simulation, the potential energy of the protein was stabilized. The final structure at 350 ps simulation was taken out from the MD trajectory and used for the docking simulation. RMSD (α -carbons) of this structure with respect to the starting energy minimized one was 2.59 Å.

Grids of probe atom interaction energies and electrostatic potential were generated by the AutoGrid program present in AutoDock 3.0. Grid spacings of 0.6 and 0.375 Å were used for the global and local searches, respectively. For each calculation, one job out of 100 docking runs was performed using a population of 200 individuals and an energy evaluation number of 3×10^6 .

NMR Experiments. NMR spectra were recorded at 298–313 K in D₂O on a Bruker Avance 500 MHz spectrometer. For the experiments with the free ligand, the compound was dissolved in D₂O, and passing argon degassed the solution. TOCSY¹⁵ and HSQC¹⁶ experiments were performed using the standard sequences. Two-dimensional T-ROESY experiments¹⁷ were performed with mixing times of 200, 300, 400, 500, and 600 ms. NOESY⁴³ cross-peaks were basically zero at room temperature and moderately positive at 313 K. The strength of the 180° pulses during the T-ROESY spin lock period was attenuated four times with respect to that of the 90° hard pulses (between 7.2 and 7.5 μ s). To deduce the interproton distances, relaxation matrix calculations were performed using software written in house, which is available from the authors upon request.⁴⁴

For the bound ligand, STD and TR-NOE experiments were performed as described⁴⁵ with a freshly prepared Peloruside A/microtubules solution. STD experiments were performed using a 20:1 ligand receptor molar ratio with 0.5, 1, and 2 s saturation time (concatenation of 50 ms Gaussian pulses). TR-NOESY experiments were performed with mixing times of 50, 100, 200, 250, and 300 ms, for a 10:1 molar ratio of ligand:protein. No purging spin lock period to remove the NMR signals of the macromolecule background was employed since they were basically not observable due to the huge size of the receptor. First, line broadening of the ligand protons was monitored after the addition of the ligand. Strong negative NOE cross-peaks were observed, in

(39) (a) Hyman, A. A.; Salser, S.; Drechsel, D. N.; Unwin, N.; Mitchison, T. J. *Mol. Biol. Cell* **1992**, *3*, 1155–1167. (b) Meurer-Grob, P.; Kasparian, J.; Wade, R. H. *Biochemistry* **2001**, *40*, 8000–8008.

(40) Oosawa, F.; Asakura, S. *Thermodynamics of the Polymerization of Protein*; Academic Press: London, 1975.

(41) Guarnieri, J.; Still, W. C. *J. Comput. Chem.* **1994**, *15*, 1302–1310.

(42) Diaz, J. F.; Kralicek, A.; Mingorance, J.; Palacios, J. M.; Vicente, M.; Andreu, J. M. *J. Biol. Chem.* **2001**, *276*, 17307–17315.

(43) Macura, S.; Ernst, R. R. *Mol. Phys.* **1980**, *41*, 95–108.

(44) Poveda, A.; Asensio, J. L.; Martín-Pastor, M.; Jiménez-Barbero, J. *J. Biomol. NMR* **1997**, *10*, 29–43.

(45) See, for instance: (a) Bernardi, A.; Potenza, D.; Capelli, A. M.; García-Herrero, A.; Cañada, F. J.; Jiménez-Barbero, J. *Chem.–Eur. J.* **2002**, *8*, 4597–4612. (b) Bernardi, A.; Arosio, D.; Manzoni, L.; Monti, D.; Posterl, H.; Potenza, D.; Mari, S.; Jiménez-Barbero, J. *Org. Biomol. Chem.* **2003**, *1*, 785–792.

contrast to the free state, indicating binding of Peloruside A to the microtubule preparation. The theoretical analysis of the TR-NOEs of the sugar protons was performed according to CORCEMA, using a relaxation matrix with exchange as described.²⁸ Different exchange rate constants were employed to obtain the optimal match between experimental and theoretical results of the intraresidue cross-peaks of the six-membered ring of Peloruside A, which has a relatively fixed geometry. Given the protein/ligand ratio, the overall correlation time, τ_c , for the free state was always set to 0.35 ns since NOESY cross-peaks for the free molecule were basically zero at room temperature and 500 MHz, and the τ_c for the bound state was set to 100 ns. To fit the experimental TR-NOE intensities, off-rate constants between 100 and 1000 s⁻¹ were tested. Optimal agreement was achieved for $k_{\text{off}} = 300 \text{ s}^{-1}$.

T-ROESY experiments were also carried out to exclude spin-diffusion effects. A continuous wave spin lock pulse was used during the 250 ms mixing time. Key NOEs were shown to be direct cross-peaks since they showed different sign to diagonal peaks.^{29,45}

Acknowledgment. We thank the Ministry of Education and Science of Spain for funding (Grants BQU2003-03550-C01 to J.J.B. and BFU2004-00358 to J.F.D.), and for a FPU Ph.D.

fellowship to R.M.B. We thank Prof. N. R. Krishna (University Birmingham, Alabama, USA) for the use of the CORCEMA program for TR-NOESY analysis, and Dr. A. Olson (Scripps Research Institute, USA) for providing AutoDock and auxiliary programs. We also thank Mr. F. Pinto (Centro de Ciencias Medioambientales, CSIC) for the microscope analysis.

Supporting Information Available: Table S1 with the NMR parameters of peloruside in D₂O solution. Figures S1 and S2 with sections of TOCSY and T-ROESY spectra of free peloruside in water solution. Figures S3 and S4 with sections of TR-NOE spectra for tubulin-bound peloruside. Figure S5 with STD data. Figure S6 with the possible rotamers of peloruside around the lateral chains. Figure S7 with the representation of polar and nonpolar areas for the major conformers of peloruside. Figure S8 showing the histogram for the docking on β -tubulin. This material is available free of charge via the Internet at <http://pubs.acs.org>.

JA0580237